Influence of Residual Stresses on the Dispersion Behavior of Guided Ultrasonic Waves in Fiber Metal Laminates

JOHANNES WIEDEMANN, TILMANN BARTH,
THOMAS ROLOFF, TOM KLUGE, NATALIE RAUTER
and CHRISTIAN HUHNE

ABSTRACT

Fiber metal laminates (FML) are a promising material as they combine the high specific properties of fiber-reinforced polymers with the ductility and damage tolerance of metals. However, during manufacturing in-plane residual stresses arise in the single layers of the laminate. The stresses mainly originate from the different coefficients of thermal expansion of the two materials and lead to an inhomogeneous stress state in the thickness direction of the FML. From homogeneous materials, it is known that stress due to external loads affects the propagation behavior of guided ultrasonic waves (GUW) in thin structures. Nevertheless, the magnitude of this effect is mode and frequency dependent. In the case of FML, the question is whether the inherent residual stresses also influence the dispersion characteristics of propagating GUW. With modified cure cycles, different residual stress states are realized in FML specimens made of carbon fiber-reinforced polymer and steel. An established measurement procedure using laser scanning vibrometry and multi-frequency excitation is used to determine the dispersion diagrams for the manufactured FML specimens. After processing the data with a non-uniform 2d discrete Fourier transform, the phase velocities over the measured frequency for the fundamental modes are compared for the different residual stress states. The results indicate that the variation of the residual stresses in the investigated FML does not show any significant effect on the GUW propagation for the measured frequencies.

INTRODUCTION

Fiber metal laminates (FML) are a material combination consisting of fiber-reinforced polymer (FRP) and metal in a layered structure. The combination is able to compensate for the brittle behavior of pure FRP materials while retaining superior specific properties compared to pure metals [1]. Due to the layered structure and the high ductility of the metal partner, FMLs show a high damage tolerance on the one hand [2]. On the other hand, impacts can lead to internal damage (e.g. delaminations) that is difficult to detect

Johannes Wiedemann, PhD Student, Email: johannes.wiedemann@tu-braunschweig.de. Technische Universitat Braunschweig, Institute of Mechanics and Adaptronics, Braunschweig, Germany

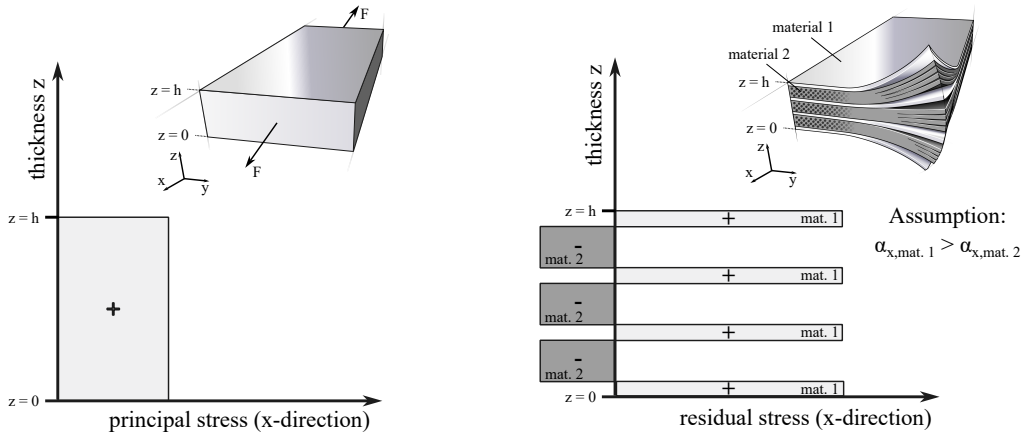

(a) Uni-axial stress state in homogeneous material (b) Residual stress state in inhomogeneous material

Figure 1. Differentiation between a uni-axial stress state due to external load in a homogeneous material like metal and manufacturing induced residual stress state in a layered material like FML

through visual inspection from the outside [3].

Structural health monitoring (SHM) using guided ultrasonic waves (GUW) is a promising approach to detect such internal damage by the interaction of the propagating waves with structural discontinuities [4]. GUWs are a type of acoustic waves that are guided by the boundaries of the structure they are propagating in. For any frequency, at least two different wave modes exist in plate-like structures which can be either symmetric or antisymmetric concerning the structure's centerline. All these modes show a frequency-dependent propagation speed.

For damage identification with GUWs, a unique correlation between damage and wave propagation is necessary. However, this is complicated, when other parameters and environmental variables also affect the wave propagation at the same time [5]. For homogeneous materials like metals, experimental investigations show that e.g. a pre-stress state is affecting the speed of propagating waves [6–8]. Whereas the influence depends on the mode and frequency considered. Such a stress state in a homogeneous material is illustrated in Figure 1a.

FMLs on the other hand exhibit an inherent residual stress state after manufacturing, which is mainly determined by the differences in the coefficients of thermal expansion (CTE) of the different layers. During the manufacturing process, the single layers are bonded at an elevated temperature of up to $180\,^{\circ}\mathrm{C}$. After the cool down of the laminate, the material layers with the greater CTE exhibit tensile stresses, while the layers of the other material exhibit compressive stresses [9]. In a typical FML the layup can get quite complex, which leads to a residual stress state that is not equally distributed over the thickness of the laminate. This is illustrated in Figure 1b.

In [10] it was shown that guided waves in FMLs are also covered by the classical solutions for wave propagation in laminated structures. The inherent residual stresses, however, raise the question of whether GUWs propagating in FMLs are also sensitive to the residual stress state inside the material. [11] indicates such an influence based on

TABLE I. Material properties for CFRP prepreg and steel [9, 13, 14]

Value	Unit	Hexcel 8552-AS4	Steel 1.4310 (X10CrNi18-8)
E_1	GPa	122	191
$E_2 = E_3$	GPa	9.9	-
$G_{12} = G_{13}$	GPa	5.2	73.5
G_{23}	GPa	3.4	-
$\nu_{12} = \nu_{13}$	-	0.27	0.3
ν_{23}	-	0.47	-
t_{ply}	mm	0.13[a]	0.12 / 0.25
α_1	ppm/K	0.4	19.0
α_2	ppm/K	31.2	-

[a] cured

numerical investigations.

To investigate the effect of the residual stresses on the wave propagation experimentally, an FML consisting of steel and uni-directional carbon fiber reinforced polymer (CFRP) is chosen. Depending on the layup, this material combination produces comparably high residual stress states.

To measure the dispersion diagrams for the manufactured FMLs, a method is chosen that has already proven to be accurate for this type of material over a large frequency range [10] which is based on a 2d discrete Fourier transformation for data evaluation. The focus is on the propagation of the two fundamental GUW modes, S_0-mode and A_0-mode in the fiber direction of the FML.

MATERIALS AND METHODS

The relevant material properties for the single materials, carbon fiber reinforced polymer (CFRP) (Hexply 8552-AS4) and a stainless steel alloy (1.4310/X10CrNi18-8) can be found in Table I, where an isotropic material behavior is assumed for the steel, although small differences in the in-plane properties have been noted in previous investigations [12].

Table I shows that the two FML constituents exhibit highly different CTEs, which will ultimately lead to the formation of a residual stress state after manufacturing. Figure 2a shows that the residual stresses in the fiber direction in the single layers highly depend on the metal volume fraction (MVF) of the laminate. A low MVF leads to high tensile stresses in the metal layers, while a high MVF increases the compressive stresses in the CFRP layers.

The residual stress state in an FML can be manipulated by modifying the temperature profile during curing, which results in different stress states independent of other material properties [9, 15]. Using such a modified cure cycle (MOD), the residual stresses can be significantly reduced compared to the manufacturer-recommended cure cycle (MRCC). The two cure cycles used in this work are shown in Figure 2b. With the MOD cycle, the temperature at which the individual layers of the laminate establish a firm bond is reduced. As a consequence, the residual stresses at room temperature are lower.

For the experiments in this work, two different MVFs are chosen to account for the

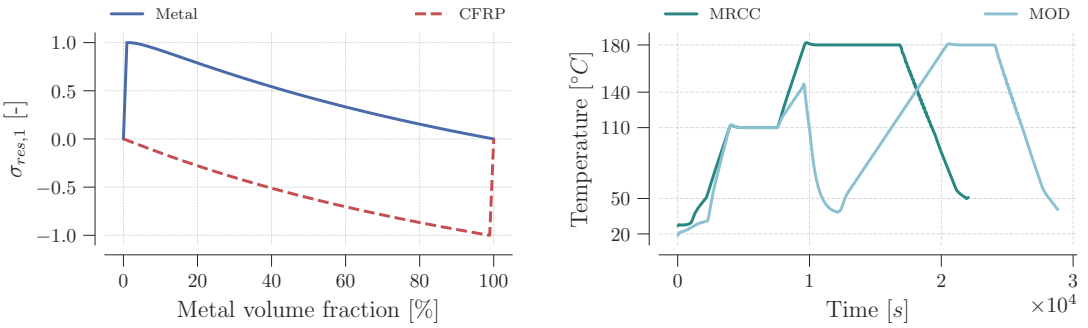

(a) Influence of MVF on residual stress

(b) Cure cycles for FML manufacturing

Figure 2. The residual stress state in FML depends on the the metal volume fraction of the laminate and the temperature profile during the manufacturing process

TABLE II. Layup of FML specimens with their respective steel ply and laminate thicknesses t and consequent metal volume fractions. Fiber layers C are oriented in 0°-direction only.

Specimen ID	Layup	t_{steel}	$t_{laminate}$	MVF
ID2	$[St/C_4/St/C_2]_S$	0.12 mm	2.04 mm	23.5 %
ID4	$[(St/\overline{C})_3]_S$	0.25 mm	2.15 mm	69.8 %

MVF influence on the residual stress state. The two laminates differ in their layup as well as the metal ply thickness to realize high MVFs and are given in Table II. For each layup, two specimens are manufactured, while one is cured with the MRCC cycle, the other specimen is cured with the MOD cycle. This will result in two different residual stress states for the specimens with the same layup.

To quantify the residual stress states in the single specimens, a method discussed in [12] is used. Therefore, additional laminates with asymmetric layups are evaluated. The asymmetric layups lead to a curvature of specimens after manufacturing. These asymmetric laminates can be reheated in an oven after final cure which results in a reduction of the curvature until a temperature is reached where the laminate is completely flat again (cf. Figure 3a). The respective temperature is known as the stress-free temperature and can subsequently serve as a reference temperature for the calculation of the residual stress state in symmetric laminates manufactured with the same manufacturing constraints. This is possible since the stress-free temperature is independent of the layup but only sensitive to extrinsic process parameters like cure cycle and tool material [12]. Therefore, in this work, the residual stress states of the FML specimens are quantified using the stress-free temperatures of asymmetric specimens manufactured with the same process parameters.

To determine the dispersion behavior of GUWs propagating in the manufactured specimens, an experimental setup with a laser scanning vibrometer is used. The setup was previously described in [10] and is depicted in Figure 3b. The measurement method uses multifrequency excitation to record the wave velocity on the specimen's surface along the measurement path. Despite the anisotropic material behavior, the wave ve-

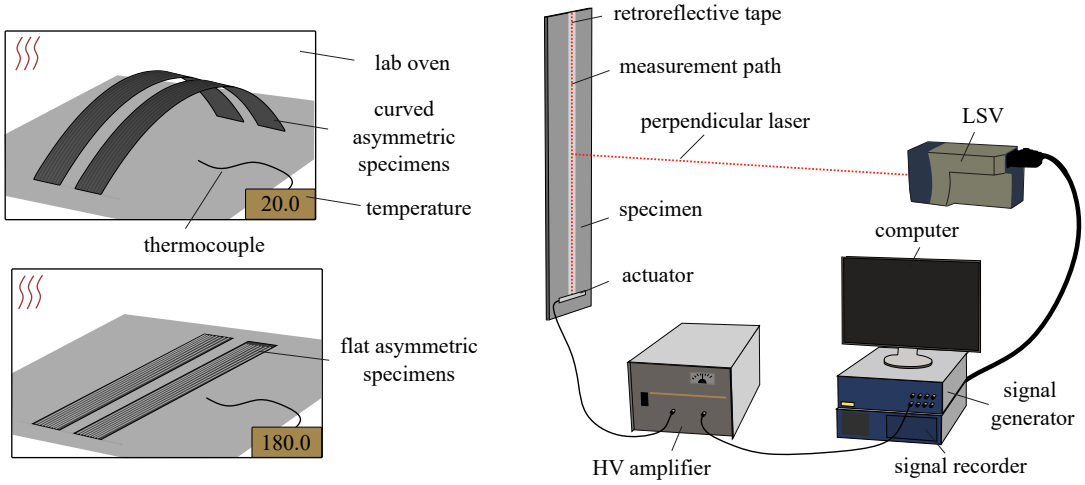

(a) Experimental setup for T_{sf} determination (b) Experimental setup for GUW measurement

Figure 3. Experimental measurement setups used in this work

locity was only measured in the direction of the uni-directional fiber orientation of the FML, since the residual stresses show the highest values in that direction. Measurements for the transverse direction can be found in e.g. [16]. The data measured in the time-spatial domain is analyzed in the frequency-wavenumber domain after applying a non-uniform discrete 2d Fourier transform. The data post-processing is also discussed in [17]. The previous investigations [10] showed that a strip-shaped specimen geometry with a width of $110\,\mathrm{mm}$ results in accurate experimental dispersion relations. Therefore, the same specimen width is chosen in this work. However, the length of the specimens is increased to $900\,\mathrm{mm}$ compared to [10] to be able to measure the wave velocities also for smaller wavenumbers.

RESULTS

By evaluating the curvature of the asymmetric laminates after manufacturing using the experimental approach shown in Figure 3a, a mean stress-free temperature of $180\,^{\circ}\mathrm{C}$ for the MRCC and $136\,^{\circ}\mathrm{C}$ for the MOD cycle is determined (cf. Table III). The standard deviation is below $3\,^{\circ}\mathrm{C}$ for both cure cycles. This results in residual stress states depending on the metal volume fraction shown in Figure 4a. For the mathematical equations using the classical laminate theory to convert stress-free temperature in residual stress states, the reader is referred to [9, 18]. The residual stress states for the two specimens ID2 and ID4 in fiber direction are shown in detail in Figure 4b. It can be seen that the residual stresses can be reduced by around $27\,\%$ using the MOD cycle. This implies a reduction of the tensile stresses in the metal plies of the ID2 specimens of around $102\,\mathrm{MPa}$ and a reduction of the compressive stresses in the CFRP layers of the ID4 specimens of around $77\,\mathrm{MPa}$ using the material properties from Table I.

The results of the dispersion measurements are shown Figure 5a and Figure 5b. The plots show the phase velocity over the frequency-thickness product. In both figures, the dispersion behavior for the fundamental A_0- and S_0-mode is plotted up to a maximum

TABLE III. Results of stress free temperature evaluation

Cure cycle	No.	Mean T_{sf} [°C]	STD [°C]
MRCC	16	180	2.7
MOD	5	136	2.9

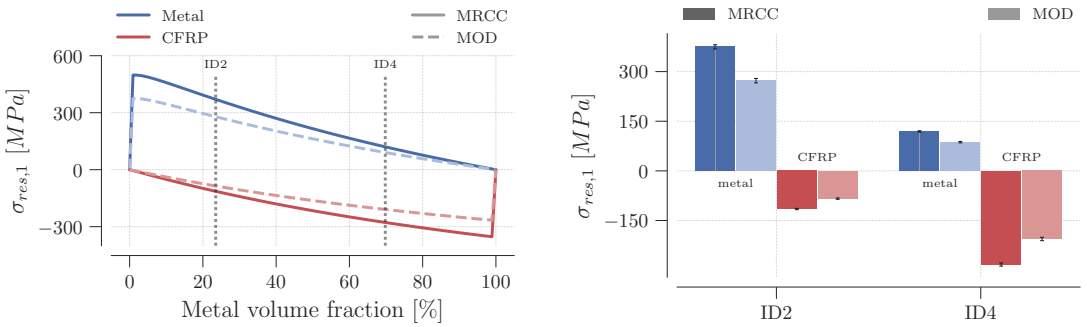

(a) (b)

Figure 4. Residual stress states for the manufactured specimens ID2 and ID4

measurement frequency of 2 kHz. However, a limitation in wavenumber exists which gives an upper and lower bound of reliable data interpretation [17]. Here, the lower limit for reliable data evaluation is set by a minimum of 20 wavelengths fitting inside the measurement path. Whereas the upper limit is given by the spatial distance between two consecutive measurement points in the measurement path. A minimum of two measurement points per wavelength is necessary. With a measurement path length of 710 mm and a spatial distance between two consecutive measurement points of around 0.9 mm, this results in the reliable data points plotted in color in the Figures 5a and 5b. The measurement points outside these wavenumber limitations are given in gray as a reference. Furthermore, some deviations in the mid-frequency range for the S_0-mode originate from the crossing of the shear-horizontal which was discussed in [10].

With these limitations in mind, the experimentally determined dispersion relations for the two stress states can be compared for ID2 and ID4. In both Figures 5a and 5b the measurement data for the high (MRCC) and low (MOD) residual stress state is presented. The results in both figures show that there are only minor deviations between the identical specimens with different residual stress states. However, these deviations can most likely be attributed to systematic variations due to the measurement procedure. By repeating measurements on an identical specimen, it could be shown that the errors lie within the same range [10].

Despite the strong variation of the residual stress state, no differences in the measured dispersion relations are observed for specimens with identical structure but different manufacturing processes. This provides a first indication that the variation of the residual stress states resulting from the cure cycle does not have a decisive influence on the dispersive behavior of the GUW. Nevertheless, follow-up studies are needed to investigate whether the mere presence of such a residual stress state has an effect on the wave propagation and whether the influences of the individual layers are comparable to

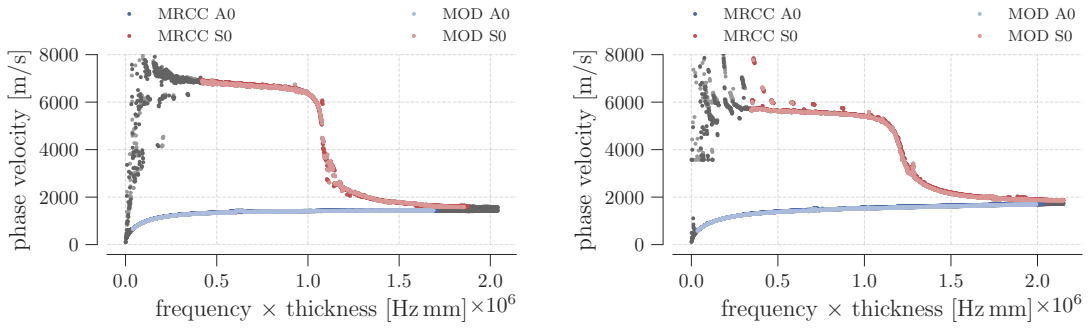

(a) ID2

(b) ID4

Figure 5. Comparison of the experimentally determined dispersion diagrams for the specimens ID2 and ID4 manufactured with the two different cure cycles MRCC and MOD

the results found in the literature for waves under pre-stress.

CONCLUSION

In this work, the influence of residual stresses in an FML made of CFRP and steel was investigated. Since the residual stress depends on the volume fractions of the two components, two different specimen layups with significantly different residual stress levels were manufactured. With cure cycle modifications, the residual stresses within an identical laminate could be decreased by around $27\,\%$. Using an established method, the dispersion diagrams for all the different FML specimens were experimentally determined over a wide frequency range with high accuracy. The comparison of the dispersion relations between the selected specimens with high and reduced residual stress states did not show any significant effect for the A_0- and S_0-mode in the investigated frequency range. In future work, these findings need to be validated using other layups and residual stress states and should be confirmed with numerical data using FEM.

ACKNOWLEDGMENT

The authors expressly acknowledge the financial support for the research work on this article within the Research Unit 3022 “Ultrasonic Monitoring of Fibre Metal Laminates Using Integrated Sensors” by the German Research Foundation (Deutsche Forschungsgemeinschaft (DFG)).

REFERENCES

1. Vlot, A. and J. W. Gunnink. 2001. *Fibre Metal Laminates: An Introduction*, Springer Netherlands, Dordrecht, ISBN 9789401009959.
2. Alderliesten, R. and J. Homan. 2006. “Fatigue and damage tolerance issues of Glare in aircraft structures,” *International Journal of Fatigue*, 28(10):1116–1123, doi:10.1016/j.ijfatigue.2006.02.015.
3. Chai, G. B. and P. Manikandan. 2014. “Low velocity impact response of fibre-metal laminates – A review,” *Composite Structures*, 107:363–381, doi:10.1016/j.compstruct.2013.08.003.

4. Giurgiutiu, V. 2008. *Structural health monitoring with piezoelectric wafer active sensors*, Academic Press/Elsevier, Amsterdam, ISBN 978-0-12-088760-6.
5. Sohn, H. 2007. "Effects of environmental and operational variability on structural health monitoring," *Philosophical transactions. Series A, Mathematical, physical, and engineering sciences*, 365(1851):539–560, doi:10.1098/rsta.2006.1935.
6. Gandhi, N., J. E. Michaels, and S. J. Lee. 2012. "Acoustoelastic Lamb wave propagation in biaxially stressed plates," *The Journal of the Acoustical Society of America*, 132(3):1284, doi:10.1121/1.4740491.
7. Qiu, L., X. Yan, X. Lin, and S. Yuan. 2019. "Multiphysics simulation method of lamb wave propagation with piezoelectric transducers under load condition," *Chinese Journal of Aeronautics*, 32(5):1071–1086, doi:10.1016/j.cja.2019.02.007.
8. Barth, T. and R. Lammering. 2023. "Numerical Investigations on the Influence of Prestress on Lamb Wave Propagation," in P. Rizzo, ed., *European Workshop on Structural Health Monitoring: EWSHM 2022 - Volume 3*, Springer, ISBN 978-3-031-07322-9.
9. Wiedemann, J., R. Prussak, E. Kappel, and C. Hühne. 2022. "In-situ quantification of manufacturing-induced strains in fiber metal laminates with strain gages," *Composite Structures*, Vol. 691(1):115967, doi:10.1016/j.compstruct.2022.115967.
10. Barth, T., J. Wiedemann, T. Roloff, T. Behrens, N. Rauter, C. Hühne, M. Sinapius, and R. Lammering, "Experimental determination of Lamb wave dispersion diagrams over large frequency ranges in fiber metal laminates: Preprint," doi:10.48550/arXiv.2206.08934.
11. Qu, J. and G. Liu. 1998. "Effects of Residual Stress on Guided Waves in Layered Media," in D. O. Thompson and D. E. Chimenti, eds., *Review of Progress in Quantitative Nondestructive Evaluation*, Springer US, Boston, MA, vol. 45, ISBN 978-1-4613-7436-7, pp. 1635–1642, doi:10.1007/978-1-4615-5339-7_212.
12. Wiedemann, J., J.-U. R. Schmidt, and C. Hühne. 2022. "Applicability of Asymmetric Specimens for Residual Stress Evaluation in Fiber Metal Laminates," *Journal of Composites Science*, 6(11):329, doi:10.3390/jcs6110329.
13. Johnston, A. A. 1997. *An integrated model of the development of process-induced deformation in autoclave processing of composite structures*, Dissertation, University of British Columbia, Vancouver, Kanada, doi:10.14288/1.0088805.
14. Kappel, E. 2020. "On thermal-expansion properties of more-orthotropic prepreg laminates with and without interleaf layers," *Composites Part C: Open Access*, 3(17):100059, doi:10.1016/j.jcomc.2020.100059.
15. Prussak, R., D. Stefaniak, E. Kappel, C. Hühne, and M. Sinapius. 2019. "Smart cure cycles for fiber metal laminates using embedded fiber Bragg grating sensors," *Composite Structures*, 213:252–260, doi:10.1016/j.compstruct.2019.01.079.
16. Barth, T., J. Wiedemann, T. Roloff, C. Hühne, M. Sinapius, and N. Rauter. 2023. "Investigations on Guided Ultrasonic Wave Dispersion Behavior in Fiber Metal Laminates Using Finite Element Eigenvalue Analysis," *Proceedings in Applied Mathematics & Mechanics*, (2), doi:10.1002/pamm.202200149.
17. Barth, T., N. Rauter, and R. Lammering. 2022. "Experimental Determination of Lamb Wave Dispersion Diagrams Using 2D Fourier Transform and Laser Vibrometry: Preprint," doi:10.21203/rs.3.rs-1321459/v1.
18. Nettles, A. T. 1994, "Basic Mechanics of Laminated composite plates: Technical Report: NASA-RP-1351," .